

HorizonNet: Learning Room Layout with 1D Representation and Pano Stretch Data Augmentation

Cheng Sun

Chi-Wei Hsiao

Min Sun

Hwann-Tzong Chen

National Tsing Hua University

{chengsun, chiweihsiao}@gapp.nthu.edu.tw

sunmin@ee.nthu.edu.tw

htchen@cs.nthu.edu.tw



Figure 1: Some examples of 3D reconstructed room layouts by our HorizonNet.

Abstract

We present a new approach to the problem of estimating 3D room layout from a single panoramic image. We represent room layout as three 1D vectors that encode, at each image column, the boundary positions of floor-wall and ceiling-wall, and the existence of wall-wall boundary. The proposed network architecture, HorizonNet, trained for predicting 1D layout, outperforms previous state-of-the-art approaches. The designed post-processing procedure for recovering 3D room layouts from 1D predictions can automatically infer the room shape with low computation cost—it takes less than 20ms for a panorama image while prior works might need dozens of seconds. We also propose Pano Stretch Data Augmentation, which can diversify panorama data and be applied to other panorama-related learning tasks. Due to the limited training data available for non-cuboid layout, we re-annotate 65 general layout data from the current dataset for fine-tuning and qualitatively show the ability of our approach to estimate general layouts.

1. Introduction

The goal of this work is to predict the room layout from a panoramic image. Most of the state-of-the-art methods

solve this problem by adopting more effective deep network architectures for their models to learn from different cues in the image. Assumptions about the room structures are often made to constrain the solution space so that the predictions of the deep model would not deviate from the common cases too much. Post-processing steps can further be performed to refine the predictions. Given a number of images with annotated layouts for training, state-of-the-art methods are able to achieve good results on the test data. However, acquiring high-quality room-layout annotations for panoramic images is labor-demanding. The annotations done by different people might be inconsistent due to ambiguities about the locations of wall boundaries especially for well-decorated rooms. Moreover, currently available datasets do not include more images of complex room layouts. The annotation for a complex layout would just be approximated as a cuboid-shaped or L-shaped layout, introducing even more ambiguities for training and testing.

Two important and correlated issues may be further addressed for improving state-of-the-art methods. The first issue is the lack of more training and validation data with precise annotations. The second issue is that, without more annotated data for training, the deep networks cannot be too large, otherwise the test accuracy might be low due to overfitting. Collecting more data to train a more sophisticated

model is indeed beneficial and doable, but a more efficient way to improve the performance should also be welcome. We argue that, if we have some better understanding of the problem and make good use of domain knowledge, we may improve the performance without acquiring a lot more annotated data or using a larger deep network. Data augmentation is a common procedure in deep learning to generate more data for training. Standard data augmentation heuristics such as random cropping or luminance change for image classification or object detection might not be effective for layout prediction. Our idea is to take account of the underlying geometric constraints and design a better data augmentation mechanism specifically for training layout-predicting deep networks. On the other hand, instead of increasing the model complexity, we aim to enhance the model by devising a compact representation with respect to the geometric constraints. We can, therefore, remove redundant degrees of freedom and force the model to focus more on learning critical properties for layout prediction.

We characterize our contributions as follows:

- We introduce a 1D $\mathcal{O}(W)$ representation that encodes the whole-room layout for a panoramic scene. Training with such a representation allows our method to outperform previous state-of-the-art results, yet requires fewer parameters and less computation time.
- We propose a data augmentation mechanism called *Pano Stretch Data Augmentation*, which generates panorama images on the fly during training and improves the accuracy under all settings in our experiments. This data augmentation mechanism also has the potential for boosting other tasks (*e.g.*, semantic segmentation, object detection) that directly work on a panorama.
- We show that leveraging RNNs in a layout prediction task is helpful for improving the accuracy. RNNs are able to capture the long-range geometric pattern of room layout.
- Owing to the 1D representation and our efficient post-processing procedure, the computation cost of our model is very low, and the model can be easily extended to handle complex scenes with layouts other than cuboid-shaped or L-shaped.

Code and all the annotated data we use in this work will be made publicly available.

2. Related Work

Room layout estimation from a single-view RGB image is an active research topic over the past decade. Many approaches have been developed in this field. Most of them

exploit the Manhattan world assumption that the room layouts, and even the furniture, are aligned with the three principal axes [3]. The Manhattan world assumption imposes constraints on the layout estimation problem, and, based on the assumption, the Manhattan aligned vanishing points could also be used to rectify the image and extract features for inferring the layout.

Delage *et al.* [6] train a dynamic Bayesian network to recognize the floor-wall boundary in each column of the perspective image. Many approaches search the Manhattan aligned layout based on extracted geometric cues. Lee *et al.* [17] test the hypothesis using Orientation Map (OM) while Hedau *et al.* [11] using Geometric Context (GC) [13]. Hedau *et al.* [9] further jointly inference the room layout with 3D objects, *e.g.* beds. Similar strategies have also been used by later methods, such as introducing an improved scoring function [25, 26], generating layout hypothesis with Manhattan junction [21], and modeling the interaction between objects and layout [5, 9, 32].

The aforementioned methods only deal with perspective images. Zhang *et al.* [30] propose to estimate the layout from a 360° H-FOV panoramic image. They extend the previous methods of vanishing point detection, hypothesis generation, and scoring hypotheses based on OM, GC and object interaction, and apply all of them to panoramas. Xu *et al.* [27] also use the OM, GC, object detection, and object orientation to reconstruct 3D layout. Yang *et al.* [28] use superpixels and Manhattan aligned line segments as features, and formulate the problem by constraint graphs. The method of [29] follows a similar approach using more geometric and semantic features. Other approaches attempt to recover the floor plan from a panorama using image gradient cues [20] or from multiple panorama images [2].

Recent methods rely more on deep networks to improve layout estimation. Most of them leverage dense prediction models to classify geometric or semantic label for each pixel. For perspective images, common ways are to predict the boundary probability map [18, 22], classes of boundaries (ceiling-wall, floor-wall, wall-wall, background) [31, 22], classes of layout surface (left, front, right, ceiling, ground) [4, 14], and corner keypoints heatmaps [16]. The predicted dense maps can be post-processed to generate layouts. A few deep learning methods have been developed for panorama-based layout estimation. Zou *et al.* [33] predict the corner probability map and boundary map directly from a panorama. They also extend Stanford 2D-3D dataset [1] with annotated layouts for training and evaluation. Fernandez-Labrador *et al.* [8] train the deep network on perspective images. During testing, they stitch the predicted perspective boundary maps into a panorama and combine them with geometric cues to infer the layout.

Unlike all the previous methods that use neural networks to perform dense prediction for layout estimation, we lever-

age the property of aligned panorama image to predict the positions of floor-wall and ceiling-wall boundaries, as well as the existence of wall-wall boundary for each column of an equirectangular image. Our model only produces three values for each column of an image, and thus the output size of the model is reduced from $\mathcal{O}(HW)$ to $\mathcal{O}(W)$. The proposed output representation is similar to [6] but they only predict floor-wall boundary for each column of a perspective image using a Dynamic Bayesian Network. In contrast, our work can handle panoramas and recognize floor-wall, ceiling-wall and wall-wall boundaries using a deep neural network. LayoutNet [33] learns to make per-pixel predictions over the entire image while our model predicts only three values for each image column. LayoutNet produces their final layout from the output of deep model by sampling. Our post-processing approach is simple and effective with time complexity = $\mathcal{O}(W)$. RoomNet [16] imitates RNN’s recurrent structure with “time steps” equal to refinement steps. We use RNN where each “time step” is responsible for estimating the result across a few image columns.

3. Approach

The goal of our approach is to estimate Manhattan room layout from a panoramic image that covers 360° H-FOV. Unlike conventional dense prediction (target output size = $\mathcal{O}(HW)$) for layout estimation using deep learning [4, 8, 7, 14, 18, 22, 31], we formulate the problem as regressing the boundaries and classifying the corner for each column of image (target output size = $\mathcal{O}(W)$). The proposed HorizonNet trained for predicting the $\mathcal{O}(W)$ target is presented in Sec. 3.1. In Sec. 3.2, we introduce a simple yet fast and effective post-processing procedure to derive the layout from output of HorizonNet. Finally in Sec. 3.3, we introduce *Pano Stretch Data Augmentation* which effectively augments the training data on-the-fly by stretching the image and ground-truth layout along x or z axis (Fig. 5).

All training and test images are pre-processed by the panoramic image alignment algorithm mentioned in [33]. Our approach exploits the properties of the aligned panoramas that the wall-wall boundaries are vertical lines under equirectangular projection. Therefore, we can use only one value to indicate the column position of wall-wall boundary instead of two (each for a boundary endpoints).

3.1. HorizonNet

Fig. 2 shows an overview of our network, which comprises a feature extractor and a recurrent neural network. The network takes a single panorama image with the dimension of $3 \times 512 \times 1024$ (channel, height, width) as input.

1D Layout Representation: The size of network output is $3 \times 1 \times 1024$. As illustrated in Fig. 3, two of the three output channels represent the ceiling-wall (y_c) and the floor-wall (y_f) boundary position of each image column, and the

other one (y_w) represents the existence of wall-wall boundary (*i.e.* corner). The values of y_c and y_f are normalized to $[-\pi/2, \pi/2]$. Since defining y_w as a binary-valued vector with 0/1 labels would make it too sparse to detect (only 4 out of 1024 non-zero values for simple cuboid layout), we set $y_w(i) = c^{dx}$ where i indicates the i th column, dx is the distance from the i th column to the nearest column where wall-wall boundary exists, and c is a constant. We set $c = 0.96$ for all our experiments. One benefit of using 1D representation is that it is less affected by zero dominant backgrounds. 2D whole-image representations of boundaries and corners would result in 95% zero values even after smoothing [33]. Our 1D boundaries representation introduces no zero backgrounds because the prediction for each component of y_c or y_f is simply a real-valued regression to the ground truth. The 1D wall-wall (corners) representation also changes the peak-background ratio of ground truth from $\frac{2N}{512 \cdot 1024}$ to $\frac{N}{1024}$ where N is the number of wall-wall corners. Therefore, the 1D wall-wall representation is also less affected by zero-dominated background. In addition, computation of 1D compact output is more efficient compared to 2D whole-image output. As depicted in Sec. 3.2, recovering the layout from our three 1D representations is simple, fast, and effective.

Feature Extractor: We adopt ResNet-50 [10] as our feature extractor. The output of each block of ResNet-50 has half spatial resolution compared to that of the previous block. To capture both low-level and high-level features, each block of the ResNet-50 contains a sequence of convolution layers in which the number of channels and the height are reduced by a factor of 8 ($= 2 \times 2 \times 2$) and 16 ($= 4 \times 2 \times 2$), respectively. More specifically, each block contains three convolution layers with $4 \times 1, 2 \times 1, 2 \times 1$ kernel size and stride, and the number of channels after each Conv is reduced by a factor of 2. All the extracted features from each layer are upsampled to the same width 256 (a quarter of input image width) and reshaped to the same height. The final concatenated feature map is of size $1024 \times 1 \times 256$. The activation function after each Conv is ReLU except the final layer in which we use Sigmoid for y_w and an identity function for y_c, y_f . We have tried various settings for the feature extractor, including deeper ResNet-101, different designs of the convolution layers after each ResNet block, and upsampling to the image width 1024, and find that the results are similar. Therefore, we stick to the simpler and computationally efficient setting.

Recurrent Neural Network for Capturing Global Information:

Recurrent neural networks (RNNs) are capable of learning patterns and long-term dependencies from sequential data. Geometrically speaking, any corner of a room can be roughly inferred from the positions of other corners; therefore, we use the capability of RNN to capture global information and long-term dependencies. Intuitively, be-

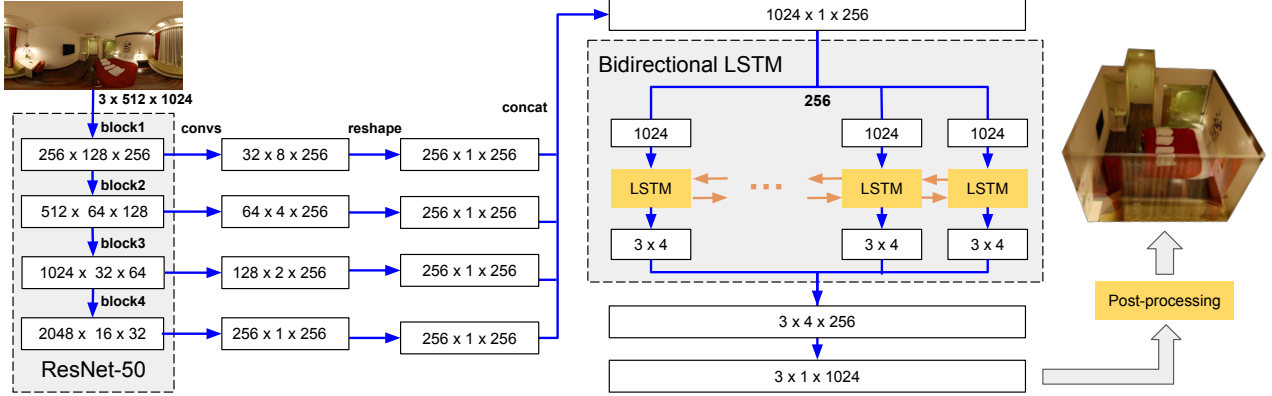


Figure 2: An illustration of the HorizonNet architecture.



Figure 3: Visualization of our 1D ground truth representations. y_w denotes the existence probability of wall-wall boundary. y_c , y_f (plotted in green and blue) denote the positions of the ceiling-wall boundary and floor-wall boundary respectively. For better visualization, we plot y_w , y_c , y_f with line width greater than one pixel.

cause LSTM [12], a type of RNN architecture, stores information about its prediction for other regions in the cell state, it has the ability to predict for occluded area accurately based on the geometric patterns of the entire room. In our model, RNN is used to predict y'_c , y'_f , y'_w column by column. That is, the sequence length of RNN is proportional to the image width. In our experiment, RNN predicts for four columns instead of one column per time step, which requires less computational time without loss of accuracy. As the y_c , y_f , y_w of a column is related to both its left and right neighbors, we adopt the bidirectional RNN [24] to capture the information from both sides. Fig. 7 and Table 1 demonstrate the difference between models with or without RNN.

3.2. Post-processing

Although the layouts reconstructed by projecting the outputs of our deep model to 3D space are very close to the ground truth layouts, they could still be improved by imposing geometric constraints or priors. LayoutNet [33] solves

the optimization problem under geometry constraints where the scoring function depends only on network outputs. The method of [8] combines outputs of their deep model with Orientation Map and Geometric Context to generate their non-cuboid layouts.

We recover general room layouts that are not limited to cuboid under following four assumptions: *i*) intersecting walls are perpendicular to each other (Manhattan world assumption); *ii*) all rooms have the one-floor-one-ceiling layout where floor and ceiling are parallel to each other; *iii*) camera height is 1.6 meters following [30]; *iv*) the pre-processing step correctly align the floor orthogonal to y -axis.

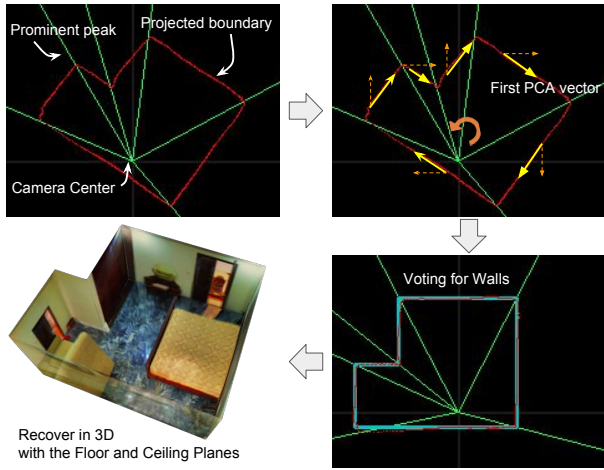
Recovering the Floor and Ceiling Planes: The distance between floor and ceiling is estimated from model output $y'_f, y'_c \in \mathcal{R}^{1024}$. We project y'_c to the reference ceiling plane and project y'_f to 3D with the same x, z coordinate as that of the corresponding y'_c position in the ceiling plane. The mean of projected floor's y coordinates decides the floor plane. We re-scale the 3D space such that the distance between the camera center and floor plane is 1.6 meters.

Recovering Wall Planes: We first find the prominent peaks on wall-wall probability $y'_w \in \mathcal{R}^{1024}$ predicted by the model. We set two criteria for prominent peaks: *i*) the signal should be larger than any other signal within 5° -FOV, and *ii*) the signal should be larger than 0.05.

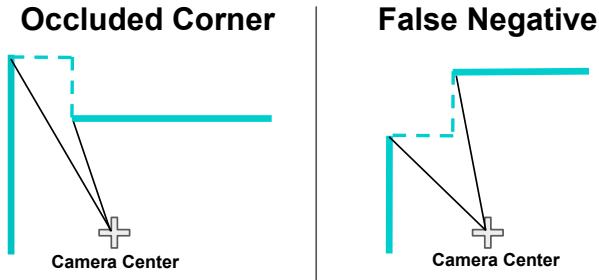
Fig. 4a shows the projected result on ceiling plane. The green lines are the detected prominent peaks which split the projected ceiling-wall boundary (red points) into multiple parts. To handle possibly failed horizontal alignment introduced from the pre-processing step, we rotate the scene based on first principal component of the projected points of each part (top right figure in Fig. 4a). We take the mean of the suggested rotation from the first principal components to correct the horizontal rotation. The variance of the distance to the principal axis also provides information about the consensus of that part, and we produce wall in an order

from low variance to high variance. We use a simple voting strategy: each projected red point votes for all planes within 0.16 meters (bottom right figure in Fig. 4a). The most voted plane is selected. Two special cases are depicted in Fig 4b which occur when the two adjacency walls are already produced and they are orthogonal to each other. After all wall planes are generated, two adjacent wall planes with the same direction are merged if their distance is less than 0.16 meter; otherwise an orthogonal wall is inserted in their midpoint. The corners are decided according to the intersection of three adjacent Manhattan junction planes.

The time complexity of our post-processing procedure is $\mathcal{O}(W)$, where W is the image width. Thus the post-processing can be efficiently done; in average, it takes less than 20ms to finish.



(a) Depicting how we recover the wall planes from our model output.



(b) Two special cases: Instead of voting for a wall, we add a corner according to the two prominent peaks and the positions of two walls.

Figure 4: Visualization of wall planes recovering. Fig. 4a is an example that the pre-processing algorithm fails to correctly align the horizontal rotation of panorama.

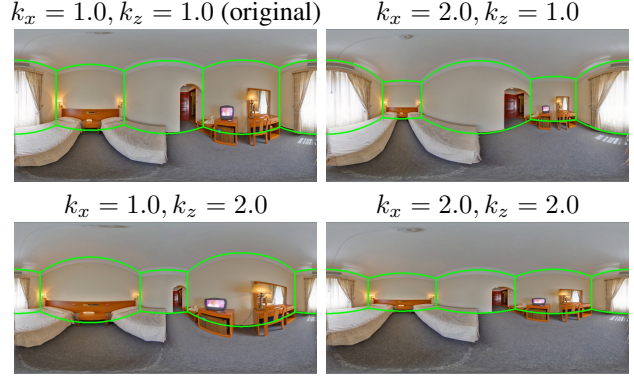


Figure 5: Visualization of the proposed *Pano Stretch Data Augmentation*. The image and ground-truth layout (green lines) are stretched along x or z axis (the effect of scaling y can be covered by x and z). This can augment the data by changing the room’s length and width. This augmentation strategy improves our quantitative results under all experiment settings (Table 2).

3.3. Pano Stretch Data Augmentation

For a 360° H-FOV panoramic image, we propose to stretch along axes in 3D space to augment training data. To achieve this goal, we first represent each pixel under UV space as (u, v) where $u \in [-\pi, \pi], v \in [-\pi/2, \pi/2]$. The coordinate (u, v) can be easily computed as the column and row of an equirectangular image, subject to a rotation angle of the camera. Here we introduce an additional variable d , which denotes the depth of a pixel. We will show that d can be eliminated later so our final equation does not depend on it.

We project the pixels to 3D space and multiply their x, y, z by k_x, k_y, k_z . The equation of stretched x', y', z' are shown in Eq. 1.

$$\begin{cases} x' = k_x \cdot x = k_x \cdot d \cdot \cos(v) \cdot \cos(u); \\ y' = k_y \cdot y = k_y \cdot d \cdot \sin(v); \\ z' = k_z \cdot z = k_z \cdot d \cdot \cos(v) \cdot \sin(u). \end{cases} \quad (1)$$

We can then project the stretched points back to the sphere by Eq. 2 for further equirectangular projection. atan2 in the equation is 2-argument arctangent. The depth d is eliminated since it exists in both terms of atan2 . We fix $k_y = 1$ because setting k_y to a value other than one is equivalent to multiplying k_x, k_z by the same value.

$$\begin{cases} u' = \text{atan2}(k_z \cdot \sin(u), k_x \cdot \cos(u)); \\ v' = \text{atan2}(k_y \cdot \sin(v), \sqrt{k_x^2 \cos^2(u) + k_z^2 \sin^2(u)} \cdot \cos(v)). \end{cases} \quad (2)$$

In our implementation, we do the inverse mapping by Eq. 3. For each pixel in the target image, we compute

the corresponding coordinate and sample its value from the source image via bilinear interpolation. Fig. 5 shows a visualization sample.

$$\begin{cases} u = \text{atan2}(k_x \cdot \sin(u'), k_z \cdot \cos(u')); \\ v = \arctan(k_z \cdot \tan(v') \cdot \csc(u') \cdot \sin(u)). \end{cases} \quad (3)$$

Note that our Pano Stretch Data Augmentation procedure could also be used on other tasks (*e.g.*, ground-truth map of semantic segmentation, bounding box for object detection) that directly work on panoramas. The augmentation procedure has the potential to boost the accuracy of those tasks.

4. Experiments

4.1. Datasets

We train and evaluate our model using the same dataset as LayoutNet [33]. The dataset consists of PanoContext dataset [30] and the extended Stanford 2D-3D dataset [1] annotated by [33]. To train our model, we generate $3 \times 1 \times 1024$ ground truth from the annotation. We follow the same training/validation/test split of LayoutNet. We train on merged training split from the PanoContext dataset and Stanford 2D-3D dataset. Likewise, we tune the hyperparameters on the merged validation split.

4.2. Training Details

The Adam optimizer [15] is employed to train the network for 300 epochs with batch size 24 and learning rate 0.0003. The L1 Loss is used for the ceiling-wall boundary (y_c) and floor-wall boundary (y_f). The Binary Cross-Entropy Loss is used for the wall-wall corner (y_w). The network is implemented in PyTorch [19]. It takes four hours to finish the training on three NVIDIA GTX 1080 Ti GPUs.

The data augmentation techniques we adopt include standard left-right flipping, panoramic horizontal rotation, and luminance change. Moreover, we propose Pano Stretch Data Augmentation (Sec. 3.3) and use it during training. For each image at each iteration, we first sample the stretching factors k_x, k_z from uniform distribution $U[1, 2]$, and then take the reciprocals of sampled values with probability 0.5. The process time of Pano Stretch Data Augmentation is roughly 130ms per 512×1024 RGB image. Therefore, it is feasible to be applied on-the-fly during training.

4.3. Cuboid Room Results

We generate cuboid room by only selecting the four most prominent peaks in the post-processing step (Sec. 3.2).

Quantitative Results: Our approach is evaluated on three standard metrics: *i*) **3D IoU**: intersection over union between 3D layout constructed from our prediction and the ground truth; *ii*) **Corner Error**: average Euclidean distance

between predicted corners and ground-truth corners (normalized by image diagonal length); *iii*) **Pixel Error**: pixel-wise error between predicted surface classes and ground-truth surface classes.

The quantitative results are summarized in Table 1. We train on both PanoContext and Stanford 2D-3D datasets, and report the testing results separately for the two datasets. This setting is also used for obtaining the best results of LayoutNet [33]. Our approach achieves state-of-the-art performance and outperforms previous methods under all the three metrics.

Qualitative Results: The qualitative results are shown in Fig. 6. We present the results from the best to the worst based on their corner errors. Please find more results in the supplemental materials.

Computation time: The 1D layout representation is easy to compute. Forward passing a single 512×1024 RGB image takes 8ms and 50ms for our HorizonNet with and without RNN respectively. The largest speed gain comes from the post-processing part. Current deep learning methods [33, 8] involve sampling in their post-processing which would take dozens of seconds. The post-processing step for our 1D representation takes only 12ms. We evaluate the result on a single NVIDIA Titan X GPU and an Intel i7-5820K 3.30GHz CPU. The reported execution time is averaged across all the testing data.

Method	3D IoU(%)	Corner error(%)	Pixel error(%)
PanoContext dataset			
PanoContext [30]	67.23	1.60	4.55
LayoutNet [33]	75.12	1.02	3.18
ours	84.23	0.69	1.90
Stanford 2D-3D dataset			
LayoutNet [33]	77.51	0.92	2.42
ours	83.51	0.62	1.97

Table 1. Quantitative results of cuboid layout estimation evaluated on the dataset organized by LayoutNet [33]. Our method outperforms the previous state-of-the-art methods under all metrics.

4.4. Ablation Study

Ablation experiments are presented in Table 2. We report the result averaged across all the testing instances. For a fair comparison, we also experiment with dense $\mathcal{O}(HW)$ prediction following LayoutNet [33] but replace the U-Net [23] with the same backbone as our architecture ¹ for a fair com-

¹To output dense (full-image) probability map, we change the Conv layer after each ResNet block from reducing both height and channels to reducing only channels, and then upsample to the same spatial dimension

Output Shape	Stretch Aug.	RNN	3D IoU(%)	Corner error(%)	Pixel error(%)	#params	FPS
dense $\mathcal{O}(HW)$			77.87	1.02	2.73	67M	98
dense $\mathcal{O}(HW)$	V		79.64	0.74	2.39	67M	98
our $\mathcal{O}(W)$			80.65	0.80	2.43	25M	119
our $\mathcal{O}(W)$	V		81.22	0.71	2.28	25M	119
our $\mathcal{O}(W)$		V	81.23	0.72	2.20	57M	20
our $\mathcal{O}(W)$	V	V	83.74	0.65	1.95	57M	20

Table 2. Ablation study demonstrates the effectiveness of each component in our approach. We show that all of our proposed designs can improve the quantitative result. Besides, our proposed 1D layout representation significantly reduces the number of parameters. FPS is measured for forward-pass of a $3 \times 512 \times 1024$ image on an NVIDIA TITAN X GPU.

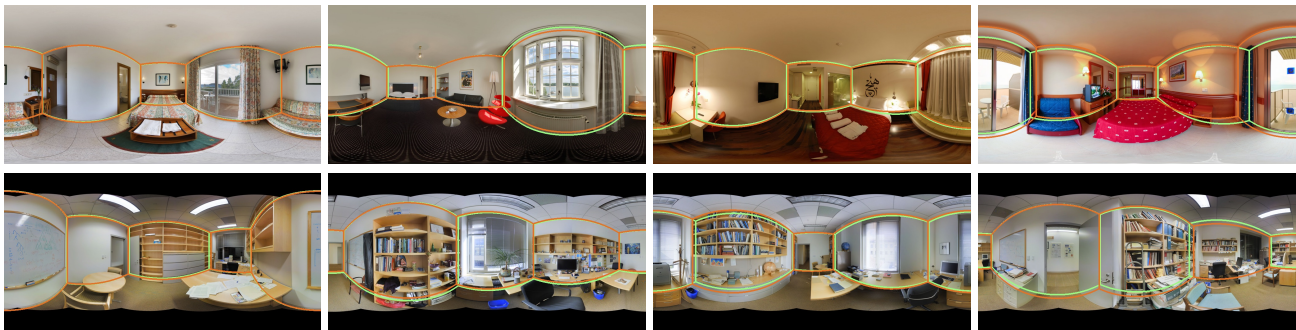


Figure 6: Qualitative results of cuboid layout estimation. The results are separately sampled from four groups that comprise results with the best 0–25%, 25–50%, 50–75% and 75–100% corner errors (displayed from the first to the fourth columns). The green lines are ground truth layout while the orange lines are estimated. The images in the first row are from PanoContext dataset [30] while second row are from Stanford 2D-3D dataset [1].

parison with the others. The results of this setting are presented in the first two rows. We do not try dense $\mathcal{O}(HW)$ output with RNN since it would consume too many computing resources. We can see that learning for the $\mathcal{O}(W)$ layout representation is better than conventional dense $\mathcal{O}(HW)$ layout representation.

We observe that training with the proposed Pano Stretch Data Augmentation can always boost the performance under all the three metrics. Note that the proposed data augmentation method can also be adopted in other tasks on panoramas and has the potential to increase their accuracy as well.

For the rows where RNN columns are unchecked, the RNN components shown in Fig 2 are replaced by fully connected layers. Our experiments show that using RNN in network architecture also improves the performance under all metrics. Fig. 7 shows some representative results with and without RNN. The raw output of the model with RNN is highly consistent with the Manhattan world even without post-processing, which demonstrates the ability of RNN to capture the geometric pattern of the entire room.

as the input image. Finally, the processed features of four blocks are con-

4.5. Non-cuboid Room Results

Since the non-cuboid rooms in PanoContext and Stanford 2D-3D dataset are labeled as cuboids, our model is never trained to recognize non-cuboid layouts and concave corners. This bias makes our model tend to predict complex rooms as cuboid. To estimate general rooms, we label 65 complex rooms from the training split to fine-tune our trained model. We keep the first Conv layer of ResNet-50 feature extractor fixed and fine-tune all the later layers for 300 epochs with learning rate $5e-5$. The batch size is set to eight and always includes four non-cuboid examples and four cuboid examples. The fine-tuning takes less than one hour on a single NVIDIA TITAN X GPU. We depict some examples of reconstructed non-cuboid layouts from the testing and validation splits in Fig.1 and Fig.8. Please find more results in the supplemental materials.

5. Conclusion

We have presented a new 1D representation for the task of room layout estimation from a panorama. The proposed

catenated and passed through a Conv layer to generate the final result.

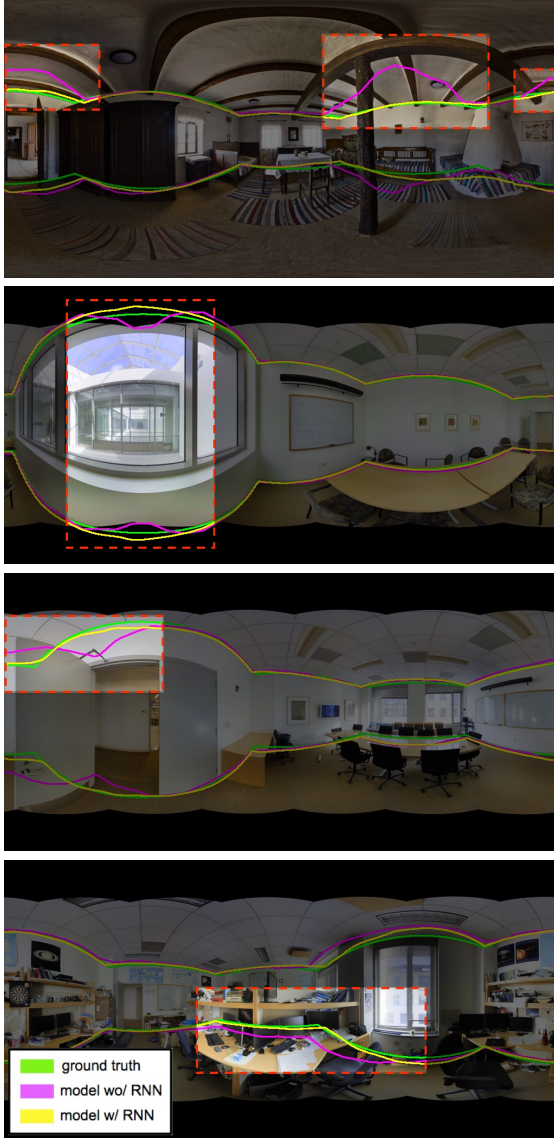


Figure 7: Visualization of model outputs with and without RNN. We plot the ground truth (green), outputs of the model with RNN (yellow), and outputs of the model without RNN (magenta). Both predictions are raw network outputs without post-processing. The model with RNN performs better than the model without RNN in images contain ceiling beam, black missing polar region caused by smaller camera V-FOV, and occluded area.

HorizonNet trained with such a representation outperforms previous state-of-the-art methods and requires less computation resource. Our post-processing method that recovers 3D layout from the model output is fast and effective, and it also works on complex room shapes even with occluded corners. The proposed Pano Stretch Data Augmentation procedure further improves our results, and can also be ap-



Figure 8: Qualitative results of non-cuboid layouts. The occluded walls are filled with black (last three 3D layouts). The blue lines in the equirectangular images are the estimated room layout boundary.

plied to the training procedure of other panorama tasks for potential improvement. We consider extending the 1D layout representation to other types of images as future work.

References

- [1] I. Armeni, A. Sax, A. R. Zamir, and S. Savarese. Joint 2D-3D-Semantic Data for Indoor Scene Understanding. *ArXiv e-prints*, Feb. 2017.
- [2] R. Cabral and Y. Furukawa. Piecewise planar and compact floorplan reconstruction from images. In *Computer Vision and Pattern Recognition (CVPR), 2014 IEEE Conference on*, pages 628–635. IEEE, 2014.
- [3] J. M. Coughlan and A. L. Yuille. Manhattan world: Compass direction from a single image by bayesian inference. In *Computer Vision, 1999. The Proceedings of the Seventh IEEE International Conference on*, volume 2, pages 941–947. IEEE, 1999.
- [4] S. Dasgupta, K. Fang, K. Chen, and S. Savarese. Delay: Robust spatial layout estimation for cluttered indoor scenes. In *Proceedings of the IEEE Conference on Computer Vision and Pattern Recognition*, pages 616–624, 2016.
- [5] L. Del Pero, J. Bowdish, B. Kermgard, E. Hartley, and K. Barnard. Understanding bayesian rooms using composite 3d object models. In *Proceedings of the IEEE Conference on Computer Vision and Pattern Recognition*, pages 153–160, 2013.
- [6] E. Delage, H. Lee, and A. Y. Ng. A dynamic bayesian network model for autonomous 3d reconstruction from a single indoor image. In *Computer Vision and Pattern Recognition, 2006 IEEE Computer Society Conference on*, volume 2, pages 2418–2428. IEEE, 2006.
- [7] C. Fernandez-Labrador, J. M. Facil, A. Perez-Yus, C. Demonceaux, and J. J. Guerrero. Panoroom: From the sphere to the 3d layout. *arXiv preprint arXiv:1808.09879*, 2018.
- [8] C. Fernandez-Labrador, A. Perez-Yus, G. Lopez-Nicolas, and J. J. Guerrero. Layouts from panoramic images with geometry and deep learning. *arXiv preprint arXiv:1806.08294*, 2018.
- [9] A. Gupta, M. Hebert, T. Kanade, and D. M. Blei. Estimating spatial layout of rooms using volumetric reasoning about objects and surfaces. In *Advances in neural information processing systems*, pages 1288–1296, 2010.
- [10] K. He, X. Zhang, S. Ren, and J. Sun. Deep residual learning for image recognition. In *2016 IEEE Conference on Computer Vision and Pattern Recognition, CVPR 2016, Las Vegas, NV, USA, June 27-30, 2016*, pages 770–778, 2016.
- [11] V. Hedau, D. Hoiem, and D. Forsyth. Recovering the spatial layout of cluttered rooms. In *Computer vision, 2009 IEEE 12th international conference on*, pages 1849–1856. IEEE, 2009.
- [12] S. Hochreiter and J. Schmidhuber. Long short-term memory. *Neural computation*, 9(8):1735–1780, 1997.
- [13] D. Hoiem, A. A. Efros, and M. Hebert. Recovering surface layout from an image. *International Journal of Computer Vision*, 75(1):151–172, 2007.
- [14] H. Izadinia, Q. Shan, and S. M. Seitz. Im2cad. In *CVPR*, 2017.
- [15] D. P. Kingma and J. Ba. Adam: A method for stochastic optimization. *CoRR*, abs/1412.6980, 2014.
- [16] C.-Y. Lee, V. Badrinarayanan, T. Malisiewicz, and A. Rabinovich. Roomnet: End-to-end room layout estimation. In *Computer Vision (ICCV), 2017 IEEE International Conference on*, pages 4875–4884. IEEE, 2017.
- [17] D. C. Lee, M. Hebert, and T. Kanade. Geometric reasoning for single image structure recovery. In *Computer Vision and Pattern Recognition, 2009. CVPR 2009. IEEE Conference on*, pages 2136–2143. IEEE, 2009.
- [18] A. Mallya and S. Lazebnik. Learning informative edge maps for indoor scene layout prediction. In *Proceedings of the IEEE international conference on computer vision*, pages 936–944, 2015.
- [19] A. Paszke, S. Gross, S. Chintala, G. Chanan, E. Yang, Z. DeVito, Z. Lin, A. Desmaison, L. Antiga, and A. Lerer. Automatic differentiation in pytorch. 2017.
- [20] G. Pintore, V. Garro, F. Ganovelli, E. Gobbetti, and M. Agus. Omnidirectional image capture on mobile devices for fast automatic generation of 2.5 d indoor maps. In *Applications of Computer Vision (WACV), 2016 IEEE Winter Conference on*, pages 1–9. IEEE, 2016.
- [21] S. Ramalingam, J. K. Pillai, A. Jain, and Y. Taguchi. Manhattan junction catalogue for spatial reasoning of indoor scenes. In *Proceedings of the IEEE Conference on Computer Vision and Pattern Recognition*, pages 3065–3072, 2013.
- [22] Y. Ren, S. Li, C. Chen, and C.-C. J. Kuo. A coarse-to-fine indoor layout estimation (cfile) method. In *Asian Conference on Computer Vision*, pages 36–51. Springer, 2016.
- [23] O. Ronneberger, P. Fischer, and T. Brox. U-net: Convolutional networks for biomedical image segmentation. In *International Conference on Medical image computing and computer-assisted intervention*, pages 234–241. Springer, 2015.
- [24] M. Schuster and K. K. Paliwal. Bidirectional recurrent neural networks. *IEEE Transactions on Signal Processing*, 45(11):2673–2681, 1997.
- [25] A. G. Schwing and R. Urtasun. Efficient exact inference for 3d indoor scene understanding. In *European Conference on Computer Vision*, pages 299–313. Springer, 2012.
- [26] R. Urtasun, M. Pollefeys, T. Hazan, and A. Schwing. Efficient structured prediction for 3d indoor scene understanding. In *2012 IEEE Conference on Computer Vision and Pattern Recognition*, pages 2815–2822. IEEE, 2012.
- [27] J. Xu, B. Stenger, T. Kerola, and T. Tung. Pano2cad: Room layout from a single panorama image. In *Applications of Computer Vision (WACV), 2017 IEEE Winter Conference on*, pages 354–362. IEEE, 2017.
- [28] H. Yang and H. Zhang. Efficient 3d room shape recovery from a single panorama. In *Proceedings of the IEEE Conference on Computer Vision and Pattern Recognition*, pages 5422–5430, 2016.
- [29] Y. Yang, S. Jin, R. Liu, S. B. Kang, and J. Yu. Automatic 3d indoor scene modeling from single panorama. In *Proceedings of the IEEE Conference on Computer Vision and Pattern Recognition*, pages 3926–3934, 2018.

- [30] Y. Zhang, S. Song, P. Tan, and J. Xiao. Panocontext: A whole-room 3d context model for panoramic scene understanding. In *European Conference on Computer Vision*, pages 668–686. Springer, 2014.
- [31] H. Zhao, M. Lu, A. Yao, Y. Guo, Y. Chen, and L. Zhang. Physics inspired optimization on semantic transfer features: An alternative method for room layout estimation. *arXiv preprint arXiv:1707.00383*, 2017.
- [32] Y. Zhao and S.-C. Zhu. Scene parsing by integrating function, geometry and appearance models. In *Proceedings of the IEEE Conference on Computer Vision and Pattern Recognition*, pages 3119–3126, 2013.
- [33] C. Zou, A. Colburn, Q. Shan, and D. Hoiem. Layoutnet: Reconstructing the 3d room layout from a single rgb image. In *Proceedings of the IEEE Conference on Computer Vision and Pattern Recognition*, pages 2051–2059, 2018.